Chinese Chemical Letters 33 (2022) 3207–3211

Contents lists available at ScienceDirect

Chinese Chemical Letters

journal homepage: www.elsevier.com/locate/cclet

Structural landscape on a series of rhein: Berberine cocrystal salt solvates: The formation, dissolution elucidation from experimental and theoretical investigations

Dezhi Yang[a,1], Hongjuan Wang[a,1], Qiwen Liu[a], Penghui Yuan[a], Ting Chen[a], Li Zhang[a], Shiying Yang[a], Zhengzheng Zhou[b,*], Yang Lu[a,*], Guanhua Du[c,*]

[a] Beijing City Key Laboratory of Polymorphic Drugs, Center of Pharmaceutical Polymorphs, Institute of Materia Medica, Chinese Academy of Medical Sciences and Peking Union Medical College, Beijing 100050, China
[b] Department of Hygiene Inspection and Quarantine Science, School of Public Health, Southern Medical University (Guangdong Provincial Key Laboratory of Tropical Disease Research, NMPA Key Laboratory for Safety Evaluation of Cosmetics), Guangzhou 510515, China
[c] Beijing City Key Laboratory of Drug Target and Screening Research, National Center for Pharmaceutical Screening, Institute of Materia Medica, Chinese Academy of Medical Sciences and Peking Union Medical College, Beijing 100050, China

ARTICLE INFO

Article history:
Received 7 September 2021
Revised 28 September 2021
Accepted 8 October 2021
Available online 14 October 2021

Keywords:
Cocrystal
Rhein
Berberine
Theoretical computation
Energy decomposition analysis
Solubility

ABSTRACT

The specific crystalline form of a compound remarkably affects its physicochemical properties. Therefore, a detailed analysis of the structural features and intermolecular interactions of a multi-component crystal is feasible to understand the relationships among the structure, physicochemical properties and the formation mechanism. In the present study, three novel cocrystal salt solvates of rhein and berberine were reported for the first time. Various solid characterizations and theoretical computations based on density functional theory (DFT) were carried out to demonstrate the intermolecular interactions. The theoretical computation shows that the strongest interaction existed between berberine cation and rhein anion, and the electrostatic interaction play a dominant role. However, no salt bond was observed between them. Further intrinsic dissolution rate analysis in water shows that the monohydrate exhibits 17 times enhancement in comparison with rhein. The rhein and berberine combined in ionic state in cocrystal salt is the main reason for the solubility improvement. This paper suggests that the interactions between the different components can be visualized and qualitatively and quantitatively analyzed by theoretical computation, which is helpful to understand the relationship between stereochemical structure and physicochemical properties of multi-component complex.

Rhein (RH) and berberine (BB) are both effective ingredients in traditional Chinese medicinal materials and have various biological activities. For example, rhein demonstrates medical activities in the treatment of inflammation, osteoarthritis, diabetes and cancer [1–4], while berberine shows its advantage in the treatment of atherosclerosis, diabetes, inflammation, and cancer [5–8]. However, these two compounds have drawbacks, in which their bioavailability is very low, limiting further clinical application. There are different reasons for the poor bioavailability of rhein and berberine. Rhein belongs to biopharmaceutics classification system (BCS) class II compound because of its poor water solubility but better permeability [9]. While, berberine hydrochloride has a relatively good solubility, its permeability is poor, and it belongs to BCS class III drug [10]. Therefore, the berberine's permeability and rhein's solubility improvements are beneficial for their bioavailability enhancement. Many complementary biological activities are associated with rhein and berberine. In some classic Chinese medicine prescriptions, traditional Chinese medicine containing rhein and berberine as active ingredients are frequently used in the compatibility, such as Sanhuang soup and Xiexin soup [11]. Therefore, a complex containing rhein and berberine should be designed to determine their complementary physicochemical properties and synergistic effect, and thus improve their bioavailability.

Based on the above consideration, we carried out studies on the organic salts (only composed of ions) of rhein and berberine (Scheme 1) [12] and accidentally obtained a series of cocrystal salt solvates. Cocrystal is a complex which consists of two or more

* Corresponding authors.
E-mail addresses: zhouzz418@smu.edu.cn (Z. Zhou), luy@imm.ac.cn (Y. Lu), dugh@imm.ac.cn (G. Du).
[1] These authors contributed equally to this work.

https://doi.org/10.1016/j.cclet.2021.10.012
1001-8417/

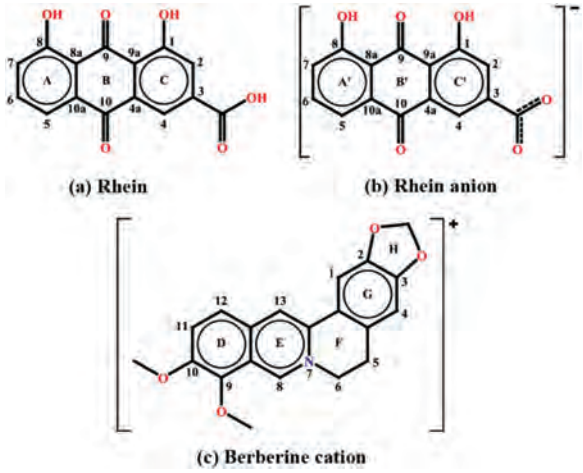

Scheme 1. Structure of (a) rhein, (b) rhein anion and (c) berberine cation.

solid state compounds linked together *via* non-covalent bonds [13–15]. It has attracted more and more attentions from pharmaceutical industries because its advantages on the physicochemical properties improvement for poorly water-soluble drugs [16–19]. According to the multicomponent crystal classification [20], cocrystal salt solvate belongs to a special class. Its components include both the molecule and ion states of drugs or coformers and the molecular states of water or solvents. Although the existence of the solvents may increase the toxicity, the importance of solvates is still reflected in their potential contributions of new crystalline forms. Some solvates exist as approved drugs on the market. Among the cocrystal salt solvates in this study, the ratio of rhein molecule: rhein anion: berberine cation: solvent molecule is 1:1:1:1, and the solvents used were water [21], methanol, ethanol and acetonitrile, respectively.

To fully understand the crystallization form, we carried out experimental characterizations, such as single crystal X-ray diffraction (SXRD), powder X-ray diffraction (PXRD), differential scanning calorimetry (DSC), and thermogravimetric (TG) analysis [22–26]. Starting from the structural characteristics of these complexes, different theoretical computations based on DFT were used to analyze the charge distribution, weak interaction, and other characteristics of their structures by using different programs [27–31], such as restrained electrostatic potential (RESP) charge distribution, atom in molecule (AIM) topological analysis, molecular electrostatic potential surface (MEPS), and energy decomposition analysis (EDA) of interaction energy. In addition, for the cocrystal salt monohydrate, intrinsic dissolution rate (IDR) analysis was used for *in vitro* evaluation [32,33].

The cocrystal salt solvates were prepared as follows: A mixture of BB chloride (1 mmol) and NaOH (1 mmol) was added into 50 mL of water and stirred for 2 h at a speed of 350 rpm. After filtration, approximately 1 mmol RH was added into the filtrate and sequentially stirred overnight. Then, the solution was filtered and left to stand at 2–8 °C for approximately 1 month. Dark red crystals were obtained. The remaining crystals including different solvents were prepared through the same process in the corresponding solvent. The detailed crystallographic information is shown in Table S1 (Supporting information). Except for BB-RH-H_2O, the other solvates were obtained for the first time. The single-crystal data were deposited in the CCDC with the reference Nos. 2107884, 2107885 and 2107886.

The main hydrogen bond interactions in the cocrystal salt solvates were similar (Fig. S1 in Supporting information). Rhein molecule and anion formed hydrogen bond interaction in $D_1^1(2)$ crystal motif. Two rhein molecules formed cyclic hydrogen bond interaction in $R_2^2(16)$crystal motifs. Intramolecular hydrogen bonding in $S_1^1(2)$ crystal motifs were found in rhein molecule and anion. However, in BB-RH-H_2O, BB-RH-MeOH, and BB-RH-EtOH, rhein anion and solvent molecule also formed hydrogen bond interaction in $D_1^1(2)$crystal motifs. In addition, no classical hydrogen or salt bond was found between rhein anion and berberine cation. π–π stacking interaction were also found in these cocrystal salt solvates and summarized in Table S2 (Supporting information).

Fig. S2 (Supporting information) shows that the experimental PXRD patterns were in line with the calculated ones. The results indicated that the prepared cocrystal salt solvates were in pure phase and could be used in other characterization experiments.

The DSC curves were similar in that they all contained a solvent endothermic peak and a complex endothermic peak, and they all showed the characteristics of melting decomposition. The solvent endothermic peak of the complexes appeared in the high temperature range of 175–194 °C, suggesting that the solvent played an important role in maintaining the crystal spatial structure and had strong interaction with other components. The second endothermic peak appeared at 224–232 °C, which was significantly lower than the endothermic peak of rhein (328 °C) and higher than that of berberine (204–206 °C). The solvent ratios of all the 4 solvates were obtained from TG analysis. The relevant TG curves are shown in green color in Fig. S3 (Supporting information). The mass loss of solvents were 1.65%, 3.23%, 4.57% and 4.29%. The number of solvents molecules in each solvate was 0.9, 0.9, 0.8 and 1.0, basically agreeing well with the SXRD results. In addition, a maximum difference of approximately 6 °C of the endothermic peak temperature was observed, which indicated significant differences existed in the arrangement of the three-dimensional space of these cocrystal salt solvates [34,35].

RESP atomic charge can effectively combine the actual situation of atomic charge in molecules dominated by electrostatic interactions [36]. Charge analysis can show the charge distribution of the cocrystal salt solvates from a whole or the ion parts and can help analyze the mechanism of the intermolecular interaction (Table S3 in Supporting information). In these cocrystal salt solvates, rhein and solvent molecules only have a small negative charge (close to zero). Rhein anion has a negative charge of −0.8 (close to −1). Berberine cations have positive charge of 0.9 (close to +1). The N atom on position 7 should have a positive charge of +1 with intuition, but it actually had only very small positive charge (close to zero). Generally, the salt bond should be formed between the positively charged N7 atom in berberine cation and carboxylate ion in rhein anion. However, the result of charge analysis showed that N7 atom had only slightly positive charge. Therefore, no salt bond existence between rhein anion and berberine cation, and they interacted with each other mainly through electrostatic interaction.

Bader's AIM topological analysis can show the characteristics of weak interaction of intra- or inter-molecules through the properties of the bond critical point (BCP) and the corresponding bond path (BP) between interacting atoms [37,38]. The BCP (orange ball) and the corresponding BP (orange line) of classical hydrogen bonds are shown clearly in Fig. 1. The BCP and BP of the non-classical hydrogen bonds such as C-H···O and C-H···C were also exhibited clearly.

The topologies of BB-RH-H_2O, BB-RH-MeOH, and BB-RH-EtOH were very similar and differed from BB-RH-ACN. BCP and BP can accurately show the intermolecular interactions as well as the intramolecular interactions in cocrystal salt solvates. Fig. 1 indicates the absence of BCP and BP between the rhein anion and berberine cation, indicating that no salt bond was present. AIM topology analysis can qualitatively show the existing interactions but cannot directly quantify the strength of the interaction. Therefore, we used MEPS and EDA to carry out additional analysis.

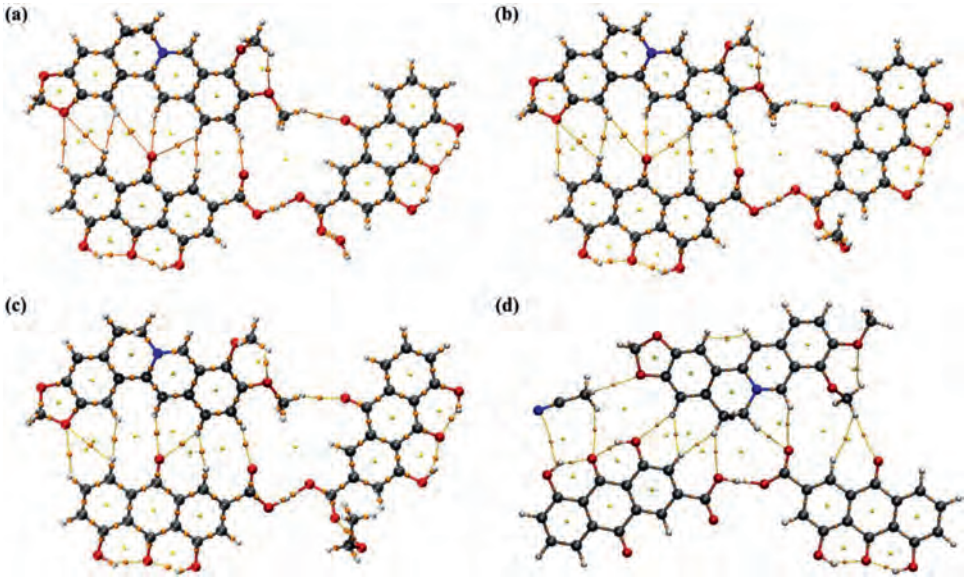

Fig. 1. AIM topological analysis of cocrystal salt solvates. (a) BB-RH-H_2O; (b) BB-RH-MeOH; (c) BB-RH-EtOH; (d) BB-RH-ACN.

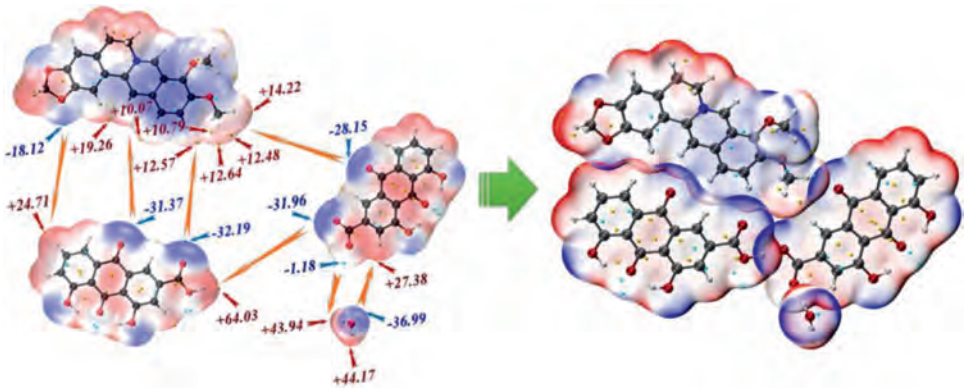

Fig. 2. MEPS analysis of cocrystal salt solvate BB-RH-H_2O.

Most of the interactions dominated by hydrogen bonds belong to electrostatic interactions, which can be demonstrated and analyzed using MEPS [39–43]. In the present paper, the color scale of the MEPS of each component in the cocrystal salt solvates was used BWR method. The blue region represents electron-rich regions. The red region represents the electron-deficient region and the white region was generally neutral. The cyan and orange ball represent the local minimum and maximum on the MEPS, respectively. Fig. 2 shows the MEPS of BB-RH-H_2O and the MEPS of the other three are show in Fig. S4 (Supporting information). The interaction sites in BB-RH-H_2O, BB-RH-MeOH, and BB-RH-EtOH were similar but quite different from BB-RH-ACN. The MEPS analysis from a spatial perspective confirmed the AIM analysis results.

EDA can decompose the total interaction energy between fragments into energy terms of physical significance to investigate the nature of the interaction [44–46]. GSK-EDA decomposes the interaction energy into five parts, as shown in Eq. 1.

$$\Delta E^{total} = \Delta E^{ele} + \Delta E^{ex} + \Delta E^{rep} + \Delta E^{pol} + \Delta E^{disp} \quad (1)$$

where ΔE^{total} is the total interaction energy of the complex, ΔE^{ele} is the electrostatic energy, ΔE^{ex} is the exchange energy, ΔE^{rep} is the repulsion energy, ΔE^{pol} is the polarization energy, and ΔE^{disp} is the electron correlation.

As listed in Table 1 and showed in Fig. S5 (Supporting information), the interaction of pair 1,2 (rhein anion and berberine cation) was basically dominated by electrostatic energy, which was the strongest interaction in these cocrystal salt solvates. The interaction of pair 1,3 (rhein anion and rhein molecule) was basically dominated by electrostatic, exchange, and polarization energy. The interaction is the second strongest interaction, which reflected the O-H···O classical hydrogen bond interaction. The interactions of pairs 1,4 (rhein anion and solvent) and 2,3 (rhein molecule and berberine cation) were much weaker than pairs 1,2 and 1,3. The interactions of pair 1,4 was basically dominated by electrostatic energy with polarization energy as secondary. The interactions of pair 2,3 were basically dominated by electrostatic energy with polarization and dispersion energy as secondary. Considering the long distance between the components of pairs 2,4 (berberine cation and water) and 3,4 (rhein molecule and solvent), no intermolecular interactions were observed between them.

EDA combined MEPS analysis can accurately explain the nature of the intermolecular interactions. For instance, no hydrogen or salt bond was found between rhein and berberine ion, but the EDA revealed that the interaction between them was the strongest and was even more than the hydrogen bond interaction between rhein and rhein ion. This finding cannot be easily explained by AIM topological analysis. Although no global maximum site is present in the MEPS of the methoxy group on position 10 of berberine cation, this region has four local maximum sites, which interacts with the carbonyl group on position 10 of rhein anion. The addition of these numbers will yield a value of approximately +50 kcal/mol. Hence, the strength of the interaction can be clearly evaluated. This phe-

Table 1
Energy decomposition in cocrystal salt solvates (kcal/mol).

Pair	ΔE^{ele}	ΔE^{ex}	ΔE^{rep}	ΔE^{pol}	ΔE^{disp}	ΔE
BB-RH-H_2O						
Pair 1,2	-39.07	-4.24	7.10	-3.19	-1.36	-40.76
Pair 1,3	-42.13	-53.87	100.60	-37.10	-4.33	-36.83
Pair 1,4	-12.52	-11.38	19.14	-4.88	-1.05	-10.69
Pair 2,3	-11.03	-14.59	24.48	-5.07	-5.19	-11.40
Pair 2,4	0.09	-0.00	0.00	-0.00	-0.01	0.08
Pair 3,4	0.56	-0.00	0.00	0.04	-0.07	0.53
Pairwise sum	-104.1	-84.08	151.32	-50.2	-12.01	-99.07
Total interaction	-103.66	-83.61	150.60	-50.34	-11.97	-98.98
Many-body effects	0.44	0.47	-0.72	-0.14	0.04	0.09
BB-RH-MeOH						
Pair 1,2	-39.04	-4.18	7.00	-3.21	-1.31	-40.74
Pair 1,3	-42.53	-55.80	104.35	-37.97	-4.38	-36.33
Pair 1,4	-16.57	-19.62	33.76	-7.64	-2.40	-12.47
Pair 2,3	-11.23	-14.99	25.18	-5.17	-5.27	-11.47
Pair 2,4	0.78	-0.00	0.00	0.06	-0.08	0.75
Pair 3,4	0.55	-0.00	0.00	0.04	-0.08	0.51
Pairwise sum	-108.04	-94.59	170.29	-53.89	-13.52	-99.75
Total interaction	-107.59	-94.05	169.44	-53.65	-13.38	-99.23
Many-body effects	0.45	0.54	-0.85	0.24	0.14	0.52
BB-RH-EtOH						
Pair 1,2	-38.45	-3.71	6.20	-3.13	-1.13	-40.22
Pair 1,3	-39.58	-50.43	93.72	-33.65	-4.33	-34.27
Pair 1,4	-11.77	-16.62	28.01	-5.52	-5.68	-11.58
Pair 2,3	-18.57	-24.40	42.04	-9.26	-3.27	-13.46
Pair 2,4	0.70	-0.00	0.00	0.04	-0.08	0.66
Pair 3,4	0.54	-0.00	0.01	0.04	-0.11	0.47
Pairwise sum	-107.13	-95.16	169.98	-51.48	-14.6	-98.40
Total interaction	-106.68	-94.65	169.11	-50.84	-14.40	-97.45
Many-body effects	0.45	0.51	-0.87	0.64	0.20	0.95
BB-RH-ACN						
Pair 1,2	-36.04	-4.48	7.52	-3.10	-0.95	-37.04
Pair 1,3	-35.83	-42.56	78.74	-27.87	-3.59	-31.11
Pair 1,4	-10.48	-12.38	20.87	-5.34	-1.64	-8.97
Pair 2,3	-10.35	-14.53	24.20	-4.59	-5.68	-10.94
Pair 2,4	1.20	-0.00	0.00	0.08	-0.12	1.17
Pair 3,4	0.63	-0.01	0.01	0.04	-0.12	0.55
Pairwise sum	-90.87	-73.96	131.34	-40.78	-12.1	-86.34
Total interaction	-90.64	-73.59	130.86	-40.78	-12.23	-86.39
Many-body effects	0.23	0.37	-0.48	0.00	-0.13	-0.05

nomenon can also be analyzed qualitatively based on the MEPS diagram. The larger the penetration distance between rhein molecule and rhein anion, the larger the repulsion energy.The smaller the penetration distance between rhein molecule and berberine cation, the smaller the repulsion energy. Although the electrostatic attraction of the former was larger, after deducting the effect of repulsion energy, the interaction of the latter was stronger.

In terms of druggability of the cocrystal salt solvates, BB-RH-H_2O was selected to investigate the dissolution rate of rhein and berberine in water. According to the IDR experiment, the dissolution rate of berberine was reduced by approximately 6 times and the dissolution amount in 60 min reduced by approximately 4 times, however the dissolution rate of rhein was increased by approximately 17 times, and the dissolution amount in 60 min increased by approximately 14 times (Fig. 3).

In this paper, four cocrystal salt solvates of rhein and berberine were prepared and characterized. To understand the structural features, we used a series of theoretical calculation methods (qualitative and quantitative) based on DFT theory to explore the interaction among these multi-component substances. This method of combining experimental characterization with theoretical calculation is significant for understanding their formation mechanism and can be used as reference the structure and physicochemical properties of other substances. RESP charge analysis can show the charge distribution of molecules and ions, and this information is helpful to evaluate salt formation. AIM topological analysis can qualitatively reveal the existence of interaction through the exis-

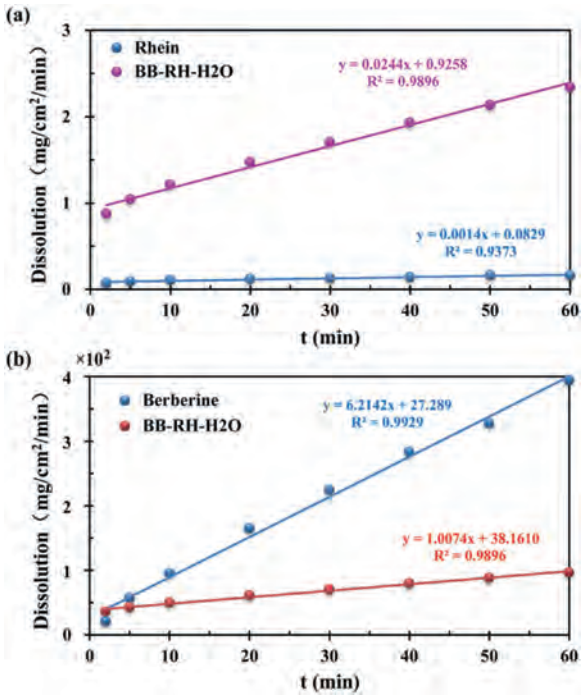

Fig. 3. IDR test for BB-RH-H_2O, rhein (a) and berberine (b) in water.

tence of BCP and BP. MEPS analysis and EDA can carry out semi-quantitative or quantitative analysis of the interaction to a certain extent. Especially, EDA can also decompose the interaction in multiple components to different components to provide a clear understanding of the nature of the interaction.

Declaration of competing interest

The authors report no declarations of interest.

Acknowledgments

We would like to express our sincere thanks to Professor Peifeng Su of Department of Chemistry, Xiamen University for providing the software developed by his research team and his help in the EDA calculation. We gratefully acknowledge the Drug Innovation Major Project (No. 2018ZX09711001-001-015), the CAMS Innovation Fund for Medical Sciences (No. 2020-I2M-1-003).

Supplementary materials

Supplementary material associated with this article can be found, in the online version, at doi:10.1016/j.cclet.2021.10.012.

References

[1] C. Shen, Z. Zhang, T. Xie, et al., Front. Pharmacol. 10 (2020) 1600.
[2] H.C. Hu, L.T. Zheng, H.Y. Yin, et al., Front. Pharmacol. 10 (2019) 1473.
[3] W. Xu, M. Hu, Q. Zhang, J. Yu, W. Su, J. Ethnopharmacol. 221 (2018) 1–9.
[4] S. Henamayee, K. Banik, B.L. Sailo, et al., Molecules 25 (2020) 2278.
[5] Y. Liu, X.J. Liu, N. Zhang, et al., Acta Pharm. Sin. B 10 (2020) 2299–2312.
[6] C.N. Li, X. Wang, L. Lei, et al., Phytother. Res. 34 (2020) 1166–1174.
[7] L. Zhu, D. Zhang, H. Zhu, et al., Atherosclerosis 268 (2018) 117–126.
[8] F. Bai, H. Tao, P. Wang, L. Wang, Y. Huang, Life Sci. 261 (2020) 118479.
[9] W. Yao, Z. Xu, J. Sun, J. Luo, J. Zou, Eur. J. Pharm. Sci. 159 (2021) 105713.
[10] M. Singh, R. Bhowal, R. Vishwakarma, D. Chopra, J. Mol. Struct. 1200 (2019) 127086.
[11] Q. Zhang, C.H. Wang, Y.M. Ma, E.Y. Zhu, Z.T. Wang, Biomed. Chromatogr. 27 (2013) 1079–1088.
[12] C. Wang, W. Sun, Z. Fang, et al., CN103319479B, 2015.
[13] M. Guo, X. Sun, J. Chen, T. Cai, Acta Pharm. Sin. B 11 (2021) 2537–2564.
[14] H. Liu, H. Lin, Z. Zhou, L. Li, Bergenin-J. Drug Deliv. Sci. Tec. 64 (2021) 102556.
[15] O.N. Kavanagh, D.M. Croker, G.M. Walker, M.J. Zaworotko, Drug Discov. Today 24 (2019) 796–804.
[16] D. Huang, H.S. Chan, Y. Wu, et al., Paeonol, J. Mol. Liq. 329 (2021) 115604.
[17] H. Liu, J. Nie, H.S. Chan, et al., Int. J. Pharmaceut. 601 (2021) 120537.
[18] F. Zhou, J. Zhou, H. Zhang, et al., J. Drug Deliv. Sci. Tec. 54 (2019) 101244.
[19] J. Zhou, L. Li, H. Zhang, et al., Int. J. Pharmaceut. 576 (2020) 118984.
[20] E. Grothe, H. Meekes, E. Vlieg, J.H. ter Horst, R. de Gelder, Cryst. Growth Des. 16 (2016) 3237–3243.
[21] X.H. Tian, P.L. Wang, T. Li, et al., Acta Pharm. Sin. B 10 (2020) 1784–1795.
[22] Agilent Technologies, CrysAlisPro, ver. 1.171.37.35, Oxfordshire, U.K., 2014.
[23] O.V. Dolomanov, L.J. Bourhis, R.J. Gildea, J.A.K. Howard, H. Puschmann, J. Appl. Crystallogr. 42 (2009) 339–341.
[24] L.J. Bourhis, O.V. Dolomanov, R.J. Gildea, J.A. Howard, H. Puschmann, Acta Crystallogr. A 71 (2015) 59–75.
[25] G.M. Sheldrick, Acta Crystallogr. C 71 (2015) 3–8.
[26] C.F. Macrae, I. Sovago, S.J. Cottrell, et al., J. Appl. Crystallogr. 53 (2020) 226–235.
[27] M.J. Frisch, G.W. Trucks, H.B. Schlegel, et al., Gaussian 16, rev. A.03, Gaussian, Inc., Wallingford CT, 2016.
[28] T. Lu, F. Chen, J. Comput. Chem. 33 (2012) 580–592.
[29] M.W. Schmidt, K.K. Baldridge, J.A. Boatz, et al., J. Comput. Chem. 14 (1993) 1347–1363.
[30] P.F. Su, Z. Jiang, Z.C. Chen, W. Wu, J. Phys. Chem. A 118 (2014) 2531–2542.
[31] P. Su, Z. Tang, W. Wu, WIRES Comput. Mol. Sci. 10 (2020) e1460.
[32] D. Yang, J. Cao, T. Heng, et al., Cryst. Growth Des. 21 (2021) 2292–2300.
[33] D. Yang, J. Cao, L. Jiao, et al., ACS omega 5 (2020) 8283–8292.
[34] Z. Zhou, H.M. Chan, H.H.Y. Sung, H.H.Y. Tong, Y. Zheng, Phytother. Res. 33 (2016) 1030–1039.
[35] Z. Zhou, M. Calatayud, J. Contreras-García, et al., J. Pharm. Sci. 108 (2019) 3340–3347.
[36] C.I. Bayly, P. Cieplak, W.D. Cornell, P.A. Kollman, J. Phys. Chem. 97 (1993) 10269–10280.
[37] R.F.W. Bader, Atoms in Molecules: A Quantum Theory, Oxford University Press, Oxford, 1990.
[38] R.F.W. Bader, Chem. Rev. 91 (1991) 893–928.
[39] J.S. Murray, P. Politzer, WIRES Comput. Mol. Sci. 1 (2011) 153–163.
[40] J.S. Murray, P. Politzer, WIRES Comput. Mol. Sci. 7 (2017) e1326.
[41] P. Politzer, J.S. Murray, Rev. Comp. Ch. 2 (1991) 273–312.
[42] Y. Luo, S. Chen, J. Zhou, et al., J. Drug Deliv. Sci. Tec. 50 (2019) 248–254.
[43] D. Yang, R. Wang, G. Jin, et al., Cryst. Growth Des. 19 (2019) 6175–6183.
[44] M.V. Hopffgarten, G. Frenking, WIRES Comput. Mol. Sci. 2 (2012) 43–62.
[45] W. Gao, H. Feng, X. Xuan, L. Chen, J. Mol. Model. 18 (2012) 4577–4589.
[46] L.L. Zhao, M.V. Hopffgarten, D.M. Andrada, G. Frenking, WIRES Comput. Mol. Sci. 8 (2017) e1345.